BIOCHEMICAL AND BIOPHYSICAL RESEARCH COMMUNICATIONS **227,** 240–247 (1996)
ARTICLE NO. 1496

Identification of Domains of the Cardiac Inward Rectifying K^+ Channel, CIR, Involved in the Heteromultimer Formation and in the G-Protein Gating

Yoshihiro Kubo*[,1] and Masaki Iizuka†

**Department of Neurophysiology, Tokyo Metropolitan Institute for Neuroscience, 2-6 Musashidai, Fuchu, Tokyo 183, Japan; and †Department of Molecular and Cellular Biology, Nippon Boehringer Ingelheim Co. Ltd, Kawanishi Pharma Research Institute, 3-10-1 Yato, Kawanishi, Hyogo 666-01, Japan*

Received September 2, 1996

The cardiac inward rectifying K^+ channel, CIR, and the strongly inward rectifying K^+ channel, IRK1, exhibited clearly different electrophysiological properties. CIR formed a heteromultimer with the G-protein coupled inward rectifying K^+ channel, GIRK1, whereas IRK1 did not, and CIR homo- and heteromultimeric channels were activated by G-protein $\beta_1\gamma_2$ subunits ($G\beta_1\gamma_2$), whereas IRK1 channels were not. To identify the domains of CIR involved in the heteromultimer formation with GIRK1 and in the $G\beta_1\gamma_2$ gating, we constructed chimeras of CIR and IRK1 and examined their electrophysiological properties. The channels were divided into three domains; the N-terminal cytoplasmic domain, the C-terminal cytoplasmic domain and the residual core domain. By the analysis, it was concluded that (i) the core region of CIR, but not the N and C cytoplasmic domains, is critical for the heteromultimer formation with GIRK1; and (ii) the N and C terminal cytoplasmic regions of CIR are sufficient for the $G\beta_1\gamma_2$ gating. We also showed that the N terminal cytoplasmic region is involved in the determination of the rate of activation upon hyperpolarization.

A cardiac inward rectifying K^+ channel, CIR, was reported to form a functional heteromultimer [1] with the G-protein coupled inward rectifying K^+ channel, GIRK1 [2]. We have also isolated a highly homologous cDNA clone to CIR from the rat and the porcine and characterized it as forming a heteromultimer with GIRK1, by qualitative and quantitative analysis of the macroscopic currents [3]. Similarly to GIRK1 homomultimers and GIRK1/CIR heteromultimers, CIR homomultimers have also been shown to be activated by $G\beta_1\gamma_2$ in the *Xenopus* oocyte expression system [1,3]. The structural basis of the assembly of channel subunits has been studied biochemically and electrophysiologically for the voltage-gated K^+ channel [4-10]. It is generally accepted that the N-terminal cytoplasmic region is critical for subfamily specific heteromultimer formation [4-6, 8-10]. In addition, Babila et al. (1994) reported that the first transmembrane region, S1, is also involved in the assembly [7]. For the inwardly rectifying K^+ channel family, it is known that some of them form functional heteromultimers [1,3,11,12,13], but the structural elements for heteromultimer formation are not known. Several recent studies have investigated the domain of GIRK1 involved in $G\beta_1\gamma_2$ gating, and the C-terminal cytoplasmic region has been shown to be critically important [14-19]. In addition, the N-terminal cytoplasmic region has also been shown to be involved [16,17]. By analogy, the cytoplasmic domains of CIR are also likely to be involved in $G\beta_1\gamma_2$ interaction, although this has not been shown experimentally. In this study, our aim was to identify the domains of CIR involved in the heteromultimer formation with GIRK1 and in the interaction with $G\beta_1\gamma_2$. As a first step, we confirmed that the strongly inward rectifying K^+ channel, IRK1 [20], does

[1] Corresponding author. Fax: 0423-21-8678. E-mail: ykubo@tmin.ac.jp.
The two authors contributed equally to this work.

0006-291X/96 $18.00

not form a heteromultimer with GIRK1, and is insensitive to $G\beta_1\gamma_2$. We constructed chimeras of CIR and IRK1, and examined which parts of CIR transferred the G-protein sensitivity and the ability to coassemble with GIRK1 to the chimera.

MATERIALS AND METHODS

Construction of chimeras. Chimeric channels were made by polymerase chain reaction (PCR) and standard molecular cloning technique. A site for Mlu1 restriction enzyme was engineered by silent mutation into the rat CIR at Asn179 [3] and into IRK1 at Asp172 [20] by PCR. These cDNAs were subcloned into the Not1-Xho1 site of pBluescript SK(−), and used to make the chimeric constructs. Chimeric fragments of the N-terminal side, C-I- (1-91 of CIR and 87-173 of IRK1) and I-C- ((1-86 of IRK1 and 92-180 of CIR), were made using the overlap extension PCR technique [21]. By replacing the corresponding regions of IRK1 (I-I-I) and CIR (C-C-C) with these chimeric fragments respectively, chimeras #1 (C-I-I) and #2 (I-C-C) were obtained. Chimeric fragments of the C-terminal side, -I (179-185 of CIR and 179-428 of IRK1) and -C (172-178 of IRK1 and 186-419 of CIR), were made by standard PCR [21]. By replacing the corresponding regions of CIR (C-C-C) and IRK1 (I-I-I) with these chimeric fragments respectively, chimeras #3 (C-C-I) and #4 (I-I-C) were obtained. Chimeras #5 and #6 were made by subcloning. Constructs with the 5′ end of CIR (C-) contained the *Xenopus* β-globin 5′-untranslated sequence at the 5′ end. Entire coding region of all constructs were confirmed by dideoxynucleotide sequencing method using a DNA sequencer (Applied Biosystems, 373A).

Electrophysiology. In vitro transcription of cRNA was as described previously [2]. Oocytes were isolated as previously described [20], and were injected with 50 nl cRNA solution at a concentration of 1 μg / ml. For IRK1, the cRNA was diluted to 30 ng/μl prior to injection. Electrophysiological recordings were carried out 3 days later at 22° ± 2° C using two-electrode voltage clamp (OC-725B-HV, Warner Co.). Data acquisition and analysis were performed on a computer using Digidata 1200 and pClamp program (Axon Instruments). Intracellular glass microelectrode were filled with 3 M KCl and the resistance was 0.3 - 0.7 Mohm. The bath solution contained 90 mM KCl, 3 mM $MgCl_2$, 5 mM HEPES (pH 7.4) and 300 μM niflumic acid.

RESULTS

Electrophysiological Properties of CIR and IRK1

The current when CIR was expressed alone, with GIRK1, or with $G\beta_1\gamma_2$ was examined electrophysiologically 3 days after cRNA injection (Fig. 1a). Oocytes injected with CIR alone (Fig. 1a) or GIRK1 alone (Fig. 1d) showed no detectable current 3 days after injection, whereas coexpression of CIR/GIRK1 or CIR/ $G\beta_1\gamma_2$ produced clearly detectable currents (Fig. 1a,e). This result suggests that CIR forms a highly functional heteromultimer with GIRK1, and that the homomultimeric channel of CIR is activated by $G\beta_1\gamma_2$.

In contrast, the current amplitude of IRK1 did not increase significantly by coexpression with GIRK1 or with $G\beta_1\gamma_2$ (Fig. 1b, e). The current traces when IRK1 and GIRK1 were coexpressed were highly similar to IRK1 current. These results demonstrate that IRK1 does not form a functional heteromultimer with GIRK1. As GIRK1 did not suppress the expression of IRK1 homomultimers (Fig. 1b, e), it indicates that GIRK1 did not form non-functional heteromultimers. It was also shown that the homomultimeric channel of IRK1 is not activated by $G\beta_1\gamma_2$ (Fig. 1b, e). Thus, CIR and IRK1 exhibit clearly different electrophysiological properties in terms of heteromultimer formation with GIRK1 and interaction with $G\beta_1\gamma_2$.

Electrophysiological Properties of Chimeras

To identify the structural elements for heteromultimeric assembly and $G\beta_1\gamma_2$ gating, chimeric channels of CIR and IRK1 were made. The channels were divided into three parts, namely the N-terminal cytoplasmic region, the core region from the beginning of M1 to the end of M2, and the C-terminal cytoplasmic region. All combinations of chimeras: chimera #1, C-I-I; chimera #2, I-C-C; chimera #3, C-C-I; chimera #4, I-I-C; chimera #5, C-I-C; chimera #6, I-C-I; were prepared by overlap extension PCR method [21].

The current of each chimera expressed either alone or with GIRK1 or with $G\beta_1\gamma_2$ was examined 3 days after cRNA injection. Examples of the current records are shown in Fig. 2 and the mean and standard deviation of the current amplitudes are shown in Fig. 3. Chimera

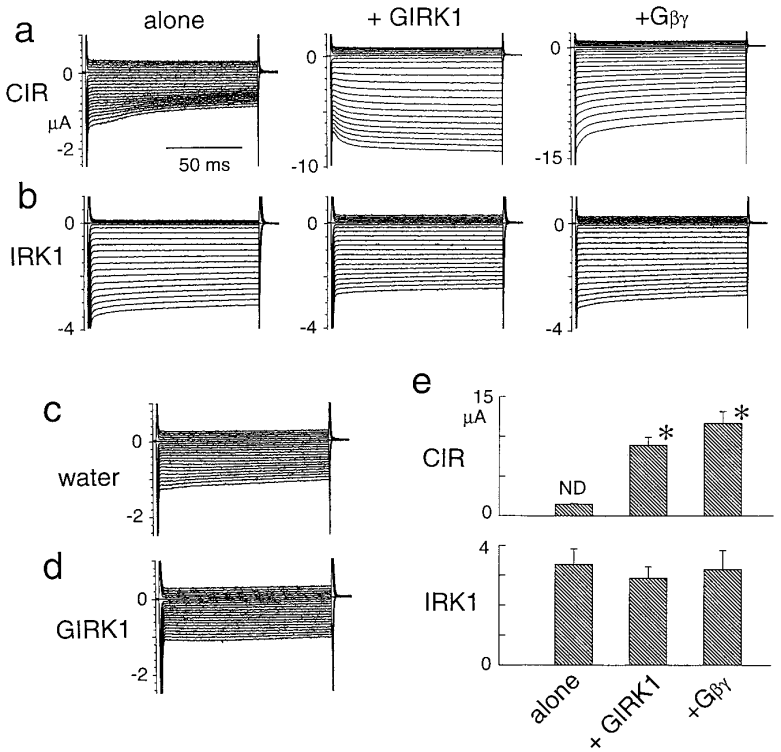

FIG. 1. Current recordings and amplitudes of CIR or IRK1 expressed in the *Xenopus* oocytes alone, with GIRK1 or with $G\beta_1\gamma_2$. (a, b) Current recordings of CIR (a) or IRK1 (b) when expressed alone (left), with GIRK1 (middle), or with $G\beta_1\gamma_2$ (right). Oocytes were voltage-clamped at 0 mV and 22 step pulses from +50 mV to −160 mV were applied. (c, d) Current traces of water (c) or GIRK1 (d) injected oocytes. Only the endogeneous current of oocyte is observed. (e) Current amplitudes of CIR or IRK1 expressed alone or with GIRK1 or with $G\beta_1\gamma_2$. The peak values at −160 mV were measured. As the endogeneous current level (ranging from 0.8 to 1.5 μA, see Fig. 1C) is not subtracted, oocyte pools which showed currents less than 1.5 μA were judged to be non-expressing, and marked ND (non-detectable). The mean, standard deviation and n values of the data obtained from the same batch of oocytes are: (CIR alone) 1.47 μA ± 0.12, n=3; (CIR with GIRK1) 8.9 ± 1.0, n=4; (CIR with $G\beta_1\gamma_2$) 11.7 ± 1.5, n=4; (IRK1 alone) 3.4 ± 0.53, n= 4; (IRK1 with GIRK1) 2.9 ± 0.34, n=4; (IRK1 with $G\beta_1\gamma_2$) 3.2 ± 0.64, n=4. The asterisks indicate data which were judged to be significantly different (p value < 0.05) from the values when expressed alone, by Student's unpaired *t*-test.

#1 (C-I-I) and #4 (I-I-C) were non functional, either when expressed alone or when co-expressed with GIRK1 or $G\beta_1\gamma_2$ (Fig. 3). Chimera #2(I-C-C) and #3 (C-C-I) did not produce detectable currents when expressed alone, but when coexpressed with GIRK1 did produce detectable currents. Coexpression of #2 or #3 with $G\beta_1\gamma_2$ did not produce detectable currents (Figs. 2a,b and 3). Chimera #5 (C-I-C) alone was non functional, but coexpression with $G\beta_1\gamma_2$ induced a clearly detectable current. By coexpressing chimera #5 and GIRK1, no current was detected (Figs. 2c and 3). Chimera #6 (I-C-I) was functional even when it was expressed alone. When coexpressed with GIRK1, the current amplitude of chimera #6 increased significantly. Coexpression of #6 with $G\beta_1\gamma_2$ did not cause any apparent changes (Figs. 2d and 3). All these results were confirmed in five different batches of oocytes.

Activation Time Constants of Heteromultimers of Chimeras with GIRK1

In the course of the analysis shown above, it was noticed that the chimeras #2 and #6, when coexpressed with GIRK1 exhibited extremely slow activation at the beginning of the

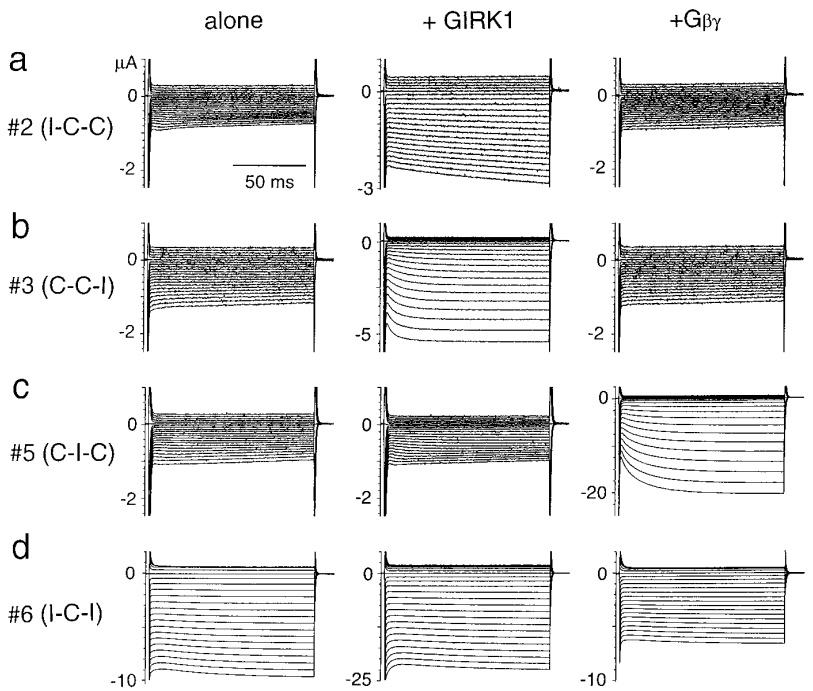

FIG. 2. Current recordings from chimeras #2 (a), #3 (b), #5 (c) and #6 (d). Each chimera was expressed in the *Xenopus* oocytes alone (left) or with GIRK1 (middle) or with $G\beta_1\gamma_2$ (right). Oocytes were voltage-clamped at 0 mV and 22 step pulses from +50 mV to −160 mV were applied.

hyperpolarizing step pulses. To examine the structural basis for this slow activation, we analyzed the activation phases of CIR and chimeras #2, 3, 6 coexpressed with GIRK1 (Fig. 4). The activation phases were fitted by the sum of two exponentials, τ_{fast} and τ_{slow}. Both τ_{fast} and τ_{slow} of chimera #2 (Fig. 4c,d) and #6 (Fig. 4g,h) were more than one order of magnitude larger than those of CIR (Fig.4a,b) and #3 (Fig. 4e,f). None of the time constants showed any voltage dependence over the range from −90 mV to −160 mV.

DISCUSSION

Heteromultimer Formation with GIRK1

A significant increase in the current amplitude by coexpression with GIRK1 was observed for chimeras #2 (I-**C**-C), #3 (C-**C**-I), # 6 (I-**C**-I) and CIR (C-**C**-C) (Fig. 3). It was not observed for chimeras #5 (C-**I**-C) and IRK1 (I-**I**-I) (Fig. 3). As chimeras #1 and # 4 were totally non-expressing (Fig. 3), it could not be determined if they were capable of forming heteromultimers with GIRK1. By comparing the structural elements of the coassembling group (#2, 3, 6 and CIR) and the non-coassembling group (#5 and IRK1), it was thought that the core region of CIR but not the cytoplasmic region is necessary and sufficient for the formation of a functional heteromultimer with GIRK1.

There is a possibility that the negative data of non-coassembling group (#5 and IRK1) were not due to lack of coassembly but due to formation of non-functional heteromultimeric channels (e.g. channels with non-conducting pore). If this is the case, it is expected that formation of non-functional heteromultimers would suppress formation of functional homomultimers. However, coexpression of GIRK1 with IRK1 did not suppress the current amplitude of IRK1 (Fig. 1b,e), suggesting that IRK1/GIRK1 heteromultimer is not only non-functional but is not formed. Similarly,

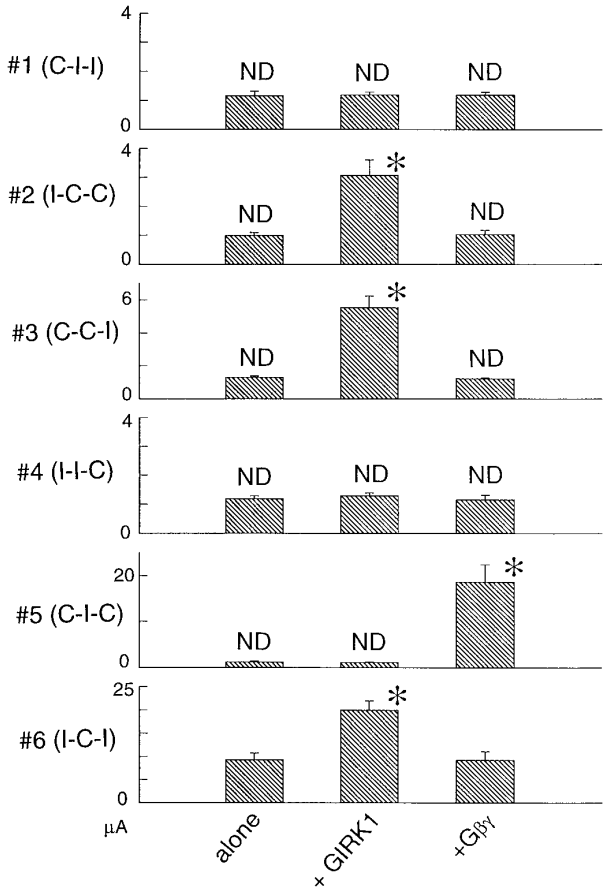

FIG. 3. Current amplitudes of chimeras #1, 2, 3, 4, 5 and 6 expressed in *Xenopus* oocytes alone (left) or with GIRK1 (right) or with $G\beta_1\gamma_2$ (right). The peak values at −160 mV were measured. As the endogeneous current level (ranging from 0.8 to 1.5 μA, see Fig. 1C) is not subtracted, oocyte pools which showed currents less than 1.5 μA were judged to be non-expressing, and marked ND (non-detectable). The mean, standard deviation and n values of the data obtained from the same batch of oocytes are: (#1 alone) 1.2 μA ± 0.15, n=3; (#1 with GIRK1) 1.2 ± 0.1, n=3; (#1 with $G\beta_1\gamma_2$) 1.2 ± 0.1, n=3; (#2 alone) 1.0 ± 0.1, n=3; (#2 with GIRK1) 3.1 ± 0.53, n=4; (#2 with $G\beta_1\gamma_2$) 1.0 ± 0.15, n=3; (#3 alone) 1.3 ± 0.1, n=3; (#3 with GIRK1) 5.5 ± 0.7, n=4; (#3 with $G\beta_1\gamma_2$) 1.2 ± 0.1, n=3; (#4 alone) 1.2 ± 0.1, n=3; (#4 with GIRK1) 1.3 ± 0.1, n=3; (#4 with $G\beta_1\gamma_2$) 1.2 ± 0.2, n=3; (#5 alone) 1.2 ± 0.2, n=3; (#5 with GIRK1) 1.1 ± 0.2, n=3; (#5 with $G\beta_1\gamma_2$) 18.6 ± 3.8, n=4; (#6 alone) 9.3 ± 1.4, n=7; (#6 with GIRK1) 20.0 ± 1.9, n=7; (#6 with $G\beta_1\gamma_2$) 9.3 ± 1.9, n=7. The asterisks indicate data which were judged to be significantly different (p value < 0.05) from the values when expressed alone, by Student's unpaired t-test.

the current amplitude of chimera #5 with $G\beta_1\gamma_2$ was not suppressed when GIRK1 was coexpressed with them (data not shown), again suggesting that chimera #5/ GIRK1 heteromultimer is not formed. Thus, we concluded that the core region is the key structural element for heteromultimeric assembly. Additionally, in a recent study with GIRK1/IRK1 chimeras, functional assembly with CIR was also seen in chimeras containing the core region of GIRK1 [17].

In the voltage-gated K^+ channel family, the structural basis for subfamily specific heteromultimerization was localized to the N-terminal cytoplasmic region [4-10]. Our present results with CIR, a member of the inward rectifying K^+ channel family, is in clear contrast to those of the voltage-gated K^+ channel family, demonstrating a difference in the mechanism of assembly of these two families.

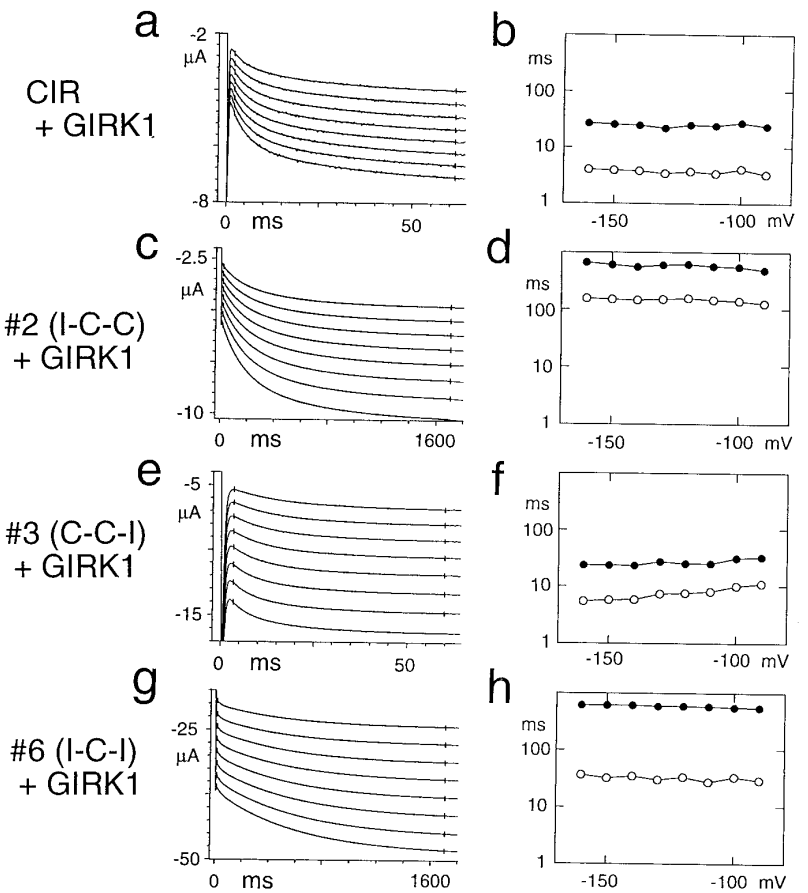

FIG. 4. Analysis of the activation phase of CIR and the chimeric molecules coexpressed with GIRK1 in *Xenopus* oocytes. Current records were fitted with the sum of two exponential (a, c, e, g), and the two activation time constants (τ_{fast} and τ_{slow}) were plotted against voltage (b, d, f, h) for CIR (a, b), chimeras #2 (c, d), #3 (e, f) and #6 (g, h). (a, c, e, g) Oocytes were voltage clamped at 0 mV and 22 step pulses from + 50 mV to −160 mV were applied. Current records from −90 mV to −160 mV were used for the reliable fitting. The range used for fitting is indicated by short vertical bars. The calculated fits are overwritten on the raw traces.

Interaction with $G\beta_1\gamma_2$

An increase in the current amplitude by coexpression with $G\beta_1\gamma_2$ was observed for chimera #5 (**C**-I-**C**) and CIR (**C**-C-**C**) (Fig. 3). It was not observed for chimera #6 (**I**-C-**I**) and IRK1 (**I**-I-**I**) (Figs. 3 and 1e). As the homomultimers of chimeras #1, 2, 3 and 4 did not produce any detectable currents when expressed alone or with $G\beta_1\gamma_2$ (Fig. 3), the possibility that they were non-expressable (e.g. these homomultimers are not properly formed in the membrane) remained. Thus, we could not determine whether chimeras #1, 2, 3 and 4 were activatable by $G\beta_1\gamma_2$ or not. By comparing the structural elements of the $G\beta_1\gamma_2$ activatable group (#5 and CIR) and the non-activatable group (#6 and IRK1), it was concluded that the N and C terminal regions of CIR are sufficient for $G\beta_1\gamma_2$ gating. If we assume that the homomultimers of chimera #2 and #3 are properly formed in the membrane, similarly to the #2/GIRK1 or #3/GIRK1 heteromultimers, then it suggests that neither chimera is gated by $G\beta_1\gamma_2$. In this case, we can conclude that both the N and C terminal cytoplasmic domains of CIR are necessary for $G\beta_1\gamma_2$ gating.

TABLE 1
The Activation Time Constants of CIR and the Chimeras #2, #3, and #6 Coexpressed with GIRK1 in *Xenopus* Oocytes

	τfast (ms) (mean and s.d., n = 4)	τslow (ms) (mean and s.d., n = 4)
CIR (C-C-C) + GIRK1	3.7 ± 0.9	25.2 ± 5.9
#2 (I-C-C) + GIRK1	156 ± 17 *	615 ± 85 *
#3 (C-C-I) + GIRK1	7.5 ± 1.7	24.5 ± 4.5
#6 (I-C-I) + GIRK1	33.5 ± 4.3 *	588 ± 71 *

The mean and standard deviation (n = 4) of τfast and τslow at −120 mV are shown. The asterisks indicate sets of data which were judged to be significantly different (p value < 0.05) by Student's unpaired t test.

The domain where $G\beta_1\gamma_2$ interacts with GIRK1 channel has been studied intensively. The functional study of the chimeras and the biochemical study of the protein-protein interaction so far showed that the C-terminal cytoplasmic region is critically involved [14-19]. In addition, it was recently reported that the N-terminal cytoplasmic region is also involved in the interaction [16,17]. The present results demonstrate that the N and C terminal cytoplasmic regions of CIR are sufficient for $G\beta_1\gamma_2$ gating. Thus, the mechanisms of $G\beta_1\gamma_2$ gating in GIRK1 and CIR appear to be similar.

Activation Kinetics

The activation kinetics of the heteromultimers of each chimera with GIRK1 exhibit obvious differences. The activation kinetics of chimera #2 (**I**-C-C) was more than one order of magnitude slower than that of CIR (**C**-C-C) (Fig. 4b,d, Table 1). Similarly, the activation kinetics of chimera #6 (**I**-C-I) was one order of magnitude slower than that of chimera #3 (**C**-C-I) (Fig. 4f,h, Table 1). These differences between chimera #2 and CIR, and #6 and #3 suggests that the N-terminal cytoplasmic region affects the kinetics of activation upon hyperpolarization.

The mechanism of the rapid activation of IRK1 was shown to be the unblocking of cytoplasmic spermine [22,23]. The binding site for spermine was identified as the Asp residue in the center of the second transmembrane region [24]. It was also reported that the C-terminal cytoplasmic region has a critical role in determining the sensitivity of the channel to the cytoplasmic blockers, suggesting some interaction between the C-terminal cytoplasmic region and the permeation pathway [25]. In contrast, the mechanism of the slow activation of the CIR/GIRK1 heteromultimer is not known. Judging from the extremely slow time course, existence of two components, and the weak voltage-dependence, the mechanism is expected to be different from that of IRK1. In the case of the GIRK1 homomultimer, it was reported that the C-terminal cytoplasmic region [26] or the Phe residue in the H5 pore region [27] is important for the slow activation. Our present results show for the first time that the N-terminal cytoplasmic region of CIR determines the speed of the slow activation of the CIR/GIRK1 heteromultimer.

ACKNOWLEDGMENTS

We thank Dr. E. L. Barsoumian for his support and encouragement throughout this project and the critical reading of the manuscript. We also thank Dr. Ruth D. Murrell-Lagnado for stimulating discussion and invaluable comments on the manuscript. Y.K. is supported by research grants from the Human Frontier Science Program Organization and the Ministry of Education, Science, Sports and Culture of Japan.

REFERENCES

1. Krapivinsky, G., Gordon, E. A., Wickman, K., Velimirovic, B., Krapivinsky, L., and Clapham, D. E. (1995) *Nature* **374,** 135–141.
2. Kubo, Y., Reuveny, E., Slesinger, P. A., Jan, Y. N., and Jan, L. Y. (1993) *Nature* **364,** 802–806.
3. Iizuka, M., Kubo, Y., Tsunenari, I., Pan, C. X., Akiba, I., and Kono, T. (1995) *Receptors and Channels* **3,** 299–315.
4. Li, M., Jan, Y. N., and Jan, L. Y. (1992) *Science* **257,** 1225–1230.
5. Shen N. V., Chen, X., Boyer, M. M., and Pfaffinger, P. J. (1993) *Neuron* **11,** 67–76.
6. Hopkins, W. F., Demas, V., and Tempel, B. L. (1994) *J. Neurosci.* **14,** 1385–1393.
7. Babila, T., Moscucci, A., Wang, H., Weaver, F. E., and Koren, G. (1994) *Neuron* **12,** 615–626.
8. Xu, J., Yu, W., Jan, Y. N., Jan, L. Y., and Li, M. (1995) *J. Biol. Chem.* **270,** 24761–24768.
9. Yu, W., Xu, J., and Li, M. (1996) *Neuron* **16,** 441–453.
10. Shen, N. V., and Pfaffinger, P. J. (1995) *Neuron* **14,** 625–633.
11. Lesage, F., Guillemare, E., Fink, M., Duprat, F., Heurteaux, C., Fosset, M., Romey, G., Barhanin, J., and Lazdunski, M. (1995) *J. Biol. Chem.* **270,** 28660–28667.
12. Velimirovic, B. M., Gordon, E. A., Lim, N. F., Navarro, B., and Clapham, D. E. (1996) *FEBS Lett.* **379,** 31–37.
13. Spauschus, A., Lentes, K-U., Wischmeyer, E., Dismann, E., Karschin, C., and Karschin, A. (1996) *J. Neurosci.* **16,** 930–938.
14. Reuveny, E., Slesinger, P. A., Inglese, J., Morales, J. M., Iniguez-Lluhi, J. A., Lefkowitz, R. J., Bourne, H. R., Jan, Y. N., and Jan, L. Y. (1994) *Nature* **370,** 143–146.
15. Takao, K., Yoshii, M., Kanda, A., Kokubun, S., and Nukada, T. (1994) *Neuron* **13,** 747–755.
16. Huang, C-L., Slesinger, P. A., Casey, P. J., Jan, Y. N., and Jan, L. Y. (1995) *Neuron* **15,** 1133–1143.
17. Slesinger, P. A., Reuveny, E., Jan, Y. N., and Jan, L. Y. (1995) *Neuron* **15,** 1145–1156.
18. Kunkel, M. T., and Peralta, E. G. (1995) *Cell* **83,** 443–449.
19. Inanobe, A., Morishige, K., Takahashi, N., Ito, H., Yamada, M., Takumi, T., Nishina, H., Takahashi, K., Kanaho, Y., Katada, T., and Kurachi, Y. (1995) *Biochem. Biophys. Res. Commun.* **212,** 1022–1028.
20. Kubo, Y., Baldwin, T. J., Jan, Y. N., and Jan, L. Y. (1993) *Nature* **362,** 127–133.
21. Horton, R. M., and Pease L. R. (1991) *in* Directed Mutagenesis (McPherson, M. J., Ed.), pp. 217–247, IRL Press, Oxford.
22. Lopatin, A. N., Makhina, E. N., and Nichols, C. G. (1994) *Nature* **372,** 366–369.
23. Fakler, B., Brandle, U., Glowatzki, E., Weidemann, S., Zenner H-P., and Ruppersberg, J. P. (1995) *Cell* **80,** 149–154.
24. Taglialatela, M., Wible, B. A., Caporaso, R., and Brown, A. M. (1994) *Science* **264,** 844–847.
25. Yang, J., Jan, Y. N., and Jan, L. Y. (1995) *Neuron* **14,** 1047–1054.
26. Pessia, M., Bond, C. T., Kavanaugh, M. P., and Adelman, J. P. (1995) *Neuron* **14,** 1039–1045.
27. Kofuji, P., Doupnik, C. A., Davidson, N., and Lester, H. A. (1996) *J. Physiol.* **490,** 633–645.